ISSN 1990-3413, Astrophysical Bulletin, 2017, Vol. 72, No. 3, pp. 232–250. © Pleiades Publishing, Ltd., 2017.
Original Russian Text © M.A. Butenko, A.V. Khoperskov, 2017, published in Astrofizicheskii Byulleten', 2017, Vol. 72, No. 3, pp. 256–275.

Galaxies with "Rows": A New Catalog

M. A. Butenko* **and A. V. Khoperskov****

Volgograd State University, Volgograd, 400062 Russia

Received November 07, 2016; in final form, June 14, 2017

Abstract—Galaxies with "rows" in Vorontsov-Velyaminov's terminology stand out among the variety of spiral galactic patterns. A characteristic feature of such objects is the sequence of straight-line segments that forms the spiral arm. In 2001 A. Chernin and co-authors published a catalog of such galaxies which includes 204 objects from the Palomar Atlas. In this paper, we supplement the catalog with 276 objects based on an analysis of all the galaxies from the New General Catalogue and Index Catalogue. The total number of NGC and IC galaxies with rows is 406, including the objects of Chernin et al. (2001). The use of more recent galaxy images allowed us to detect more "rows" on average, compared with the catalog of Chernin et al. When comparing the principal galaxy properties we found no significant differences between galaxies with rows and all S-type NGC/IC galaxies. We discuss two mechanisms for the formation of polygonal structures based on numerical gas-dynamic and collisionless N-body calculations, which demonstrate that a spiral pattern with rows is a transient stage in the evolution of galaxies and a system with a powerful spiral structure can pass through this stage. The hypothesis of A. Chernin et al. (2001) that the occurrence frequency of interacting galaxies is twice higher among galaxies with rows is not confirmed for the combined set of 480 galaxies. The presence of a central stellar bar appears to be a favorable factor for the formation of a system of "rows".

DOI: 10.1134/S1990341317030130

Key words: *galaxies: spiral—galaxies: statistics—galaxies: structure*

1. INTRODUCTION

Straight-line segments that form the spiral pattern can be seen in the images of some spiral galaxies. Vorontsov-Velyaminov [1] must be the first to point out this feature, calling the said segments "rows". Such rather long and practically straight-line segments form uneven, but almost regular spiral arms, and these structures are often called polygonal arms [2]. The M101 and M51 galaxies are typical examples. A. D. Chernin with coauthors compiled a catalog of galaxies with "rows" including 204 objects [3, 4]. An analysis of such structures revealed that they have the following properties [3]:

1. The length L of the straight-line segment ("row") linearly increases with galactocentric distance d, $d = (1.00 \pm 0.11)L$.
2. The angle between the two adjacent segments is close to $\alpha = 120°$ (with a standard deviation of 10°).
3. Straight-line segments can be subdivided into two types: those that form rather regular global structure of the spiral arm and one–two segments that do not form the global spiral pattern.
4. "Rows" are observed mostly in galaxies of late morphological types Sbc–Scd.
5. Straight-line segments occur more often in interacting galaxies.
6. The average number of "rows" in a galaxy is $N = 3$.
7. Galaxies with "rows" are rather rare objects making up for about 7% of all spiral galaxies with well-defined spiral arms.

Note that these results are based on an analysis of photographic plates and Palomar Atlas images.

In this paper we report the results of an analysis of our catalog of galaxies with polygonal structures, which lists 276 objects not included into the earlier published catalog [3]. When combined, these catalogs include all NGC and IC galaxies with "rows".

2. SAMPLE OF GALAXIES WITH "ROWS"

2.1. General Characterization

When searching for galaxies with "rows" (straight-line arm segments) we inspected more than 30 000

*E-mail: maria_butenko@volsu.ru
**E-mail: khoperskov@volsu.ru

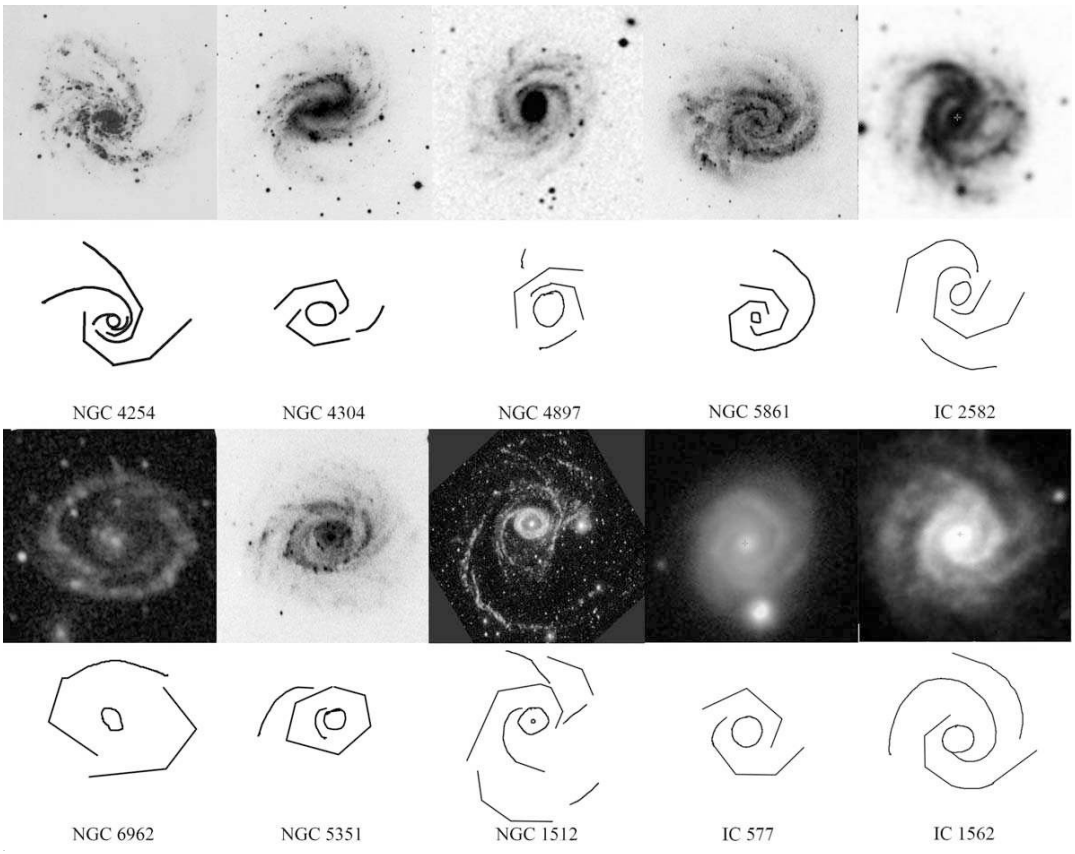

Fig. 1. Examples of galaxies with "rows" forming various geometric structures.

images of spiral galaxies taken in different parts of the spectrum and adopted from astronomical databases. This includes all spiral galaxies in the NGC/IC catalogs. Our analysis revealed 276 galaxies with straight-line segments in addition to the 204 galaxies with "rows" listed in the catalog of Chernin et al. [3]. We imposed the following additional constraints: declination $\delta > -45°$, objects should be brighter than $15^{\rm m}$, inclination of the galaxy to the line of sight $i < 70°$, distance less than 200 Mpc, and $R_{25} \lesssim 30$ kpc. When compiling our sample we used images from all available sources including DSS, SDSS, GALEX, 2MASS, and HST. We show some examples of galaxies with "rows" in Fig. 1. We also identify so-called hexagonal structures [2, 5], which form almost ring-like features in the galactic disk (NGC 4736, NGC 5351, NGC 6962, NGC 7329, IC 1764, IC 4688).

In some objects polygons can be detected in various spectral ranges, however, there are exceptions. Polygonal structures in 2MASS images could be found only in the NGC 4254, NGC 5156, NGC 5351, NGC 5653, NGC 5968, NGC 6035, NGC 6691, NGC 7678, IC 1142, IC 2627, IC 4219, IC 4359, IC 4444, IC 4567, IC 4646, IC 4836, IC 4839, and IC 5325 galaxies.

We performed primary selection by examining galaxy images from astronomical databases. We then processed the images of such galaxies as described in [6]. We transformed the image of a galaxy with rows to the "face-on" form ($i \approx 0$) by rotating it for the major axis to coincide with one of the coordinate axis and stretching the image along the direction of the minor axis assuming that the disk is infinitely thin. We then superimposed onto the transformed galaxy image lines tracing the geometry of "rows". We then determined for each galaxy: the length L_i of ith "row", distance d_i from the galactic center to the edge of the "row", and angle α_i between the adjacent straight-line segments.

To estimate the error of this method, we performed series of simulations by taking pictures of schematic images of various polygonal structures at different angles i and transforming such images to the "face-on" form.

At fixed i the errors of L and α estimates depend strongly on the geometry of the polygonal structure and the location of the particular "row" in the plane perpendicular to the line of sight. Depending on the location of "rows" the error of estimated L and α lies within $0 \leqslant \varepsilon \leqslant \varepsilon_{\max}$. Our simulations yield $\varepsilon^{(L)}_{\max} = 12\%$ and $\varepsilon^{(\alpha)}_{\max} = 6\%$ for $i = 60°$, decreasing

down to $\varepsilon_{\max}^{(L)} = 9\%$ and $\varepsilon_{\max}^{(\alpha)} = 3\%$ for $i = 30^\circ$. In the case of random location and orientation of the "row" the error of its parameter estimates is of about $\varepsilon_{\max}/2$. When averaged over all simulations and all "rows" the error does not exceed 5% for linear measurements. A similar averaging for angles yields $\delta\alpha \approx 3\%$. Hence within the framework of the above approach the errors of linear and angle parameters do not exceed the errors of initial observational data even if "rows" are identified by eye.

As a result, we found 276 objects in addition to those listed in the catalog of Chernin et al. [3]. Table 1 gives the following information about our newly discovered objects: (1) name of the galaxy according to NGC or IC; (2) morphological type; (3) integrated B_0 magnitude corrected for Galactic extinction and inclination to the line of sight; (4) heliocentric radial velocity V_0; (5) absolute magnitude M_B (computed with $H_0 = 75\,\mathrm{km\,s^{-1}\,Mpc^{-1}}$); (6) H I mass-to-luminosity ratio $M_{\mathrm{H\,I}}/L_B$ (in solar units); (7) number of "rows" found in the galaxy; (8) reference to the main image of the galaxy where the straight-line segments of the spiral structure were found that was used to count their number, measure the linear size and angles between the "rows"; (9) references to other images where straight-line "rows" can be found, and (10) information about whether the galaxy exhibits any signs of interaction. The parameter values listed in columns (2)–(6) of Table 1 are adopted from HyperLeda (See [7] and `http://leda.univ-lyon1.fr/`).

Note that unlike the sample constructed by Chernin et al. [3], only 12 of our selected 276 galaxies are mentioned in the Catalog of interacting galaxies of Vorontsov-Velyaminov (VV). Several more galaxies have spiral patterns with a characteristic perturbed stricture or signs of strong interactions in the past (e.g., NGC 0060, NGC 1068, NGC 2442, NGC 5774, IC 1142, IC 2956 and IC 4441, and IC 4567). When analyzing our sample we used, in addition to the VV catalog, the catalog of peculiar galaxies (ARP), tidal index estimates for Local group galaxies [8, 9], and information from the HyperLeda database, namely, the *multiple* parameter, which is equal to *M* if the object belongs to a group. The small fraction of interacting galaxies in our sample may be due to the fact that objects with the most conspicuous signs of interaction have already been included into the catalog of A. D. Chernin et al. [3].

Table 1. Galaxies with "rows"

NGC/IC	Type	B_0	V_0, km s^{-1}	M_B	M_{HI}/L_B	Number of "row"	Main Reference*	Other References*	Inter-action**
(1)	(2)	(3)	(4)	(5)	(6)	(7)	(8)	(9)	(10)
0010	Sbc	12.74	6803	−22.18	0.18	5	B	C, R	
0060	Sc	14.66	11809	−21.52		5	SD	B	asym
0099	Sc	13.71	5310	−20.74	0.86	3	B	SD	
0157	SABb	10.40	1654	−21.41	0.17	4	SD	B	
0165	Sbc	13.50	5889	−21.13	0.29	5	G	B	
0191	SABc	13.75	6076	−20.96		4	SD	B	ARP 127
0201	Sc	13.35	4386	−20.66	0.25	4	SD	B	M
0214	SABc	12.49	4535	−21.65	0.14	5	HST	SD, B	
0234	SABc	12.91	4449	−21.16	0.21	9	SD	C, B	
0255	Sbc	12.21	1597	−19.55	0.73	3	B	C	
0268	Sbc	13.00	5479	−21.49	0.46	2	SD	B	
0289	SBbc	11.39	1630	−20.25	1.16	2	G	B	VV 484, M, Grp
0300	Scd	8.40	165	−18.14	1.59	6	G	B	
0521	Sbc	12.40	5023	−21.90	0.15	6	SD	B, C	
0578	Sc	11.11	1628	−20.59	0.33	3	B	C	

Table 1. (Contd.)

NGC/IC	Type	B_0	V_0, km s^{-1}	M_B	M_{HI}/L_B	Number of "row"	Main Reference*	Other References*	Inter-action**
(1)	(2)	(3)	(4)	(5)	(6)	(7)	(8)	(9)	(10)
0685	Sc	11.58	1360	−19.45	0.63	1	B	C, R	
0753	SABc	12.32	4902	−21.99	0.30	7	B	C	
0783	Sc	12.43	5192	−22.01	0.14	4	G	SD, B, C	
0799	SBa	13.96	5837	−20.66	0.31	2	SD	B, C	
0800	Sc	14.03	5934	−20.63	0.38	2	SD	B	
0877	SABc	11.83	3913	−21.95	0.30	5	B	G, C	
0887	SABc	13.02	4311	−20.88	0.44	1	B	G, C, R	
0895	Sc	11.88	2288	−20.67	0.50	5	SD	G, B, C	
0925	Scd	9.78	554	−20.17	0.25	5	B	G, C	
0977	Sa	13.85	4611	−20.22	0.43	4	B	G, C	
0986	Sab	11.44	1984	−20.62	0.09	2	B	G, C	
1068	Sb	9.53	1138	−21.50	0.04	4	G	B	ARP 037, Grp
1073	SBc	11.16	1208	−20.02	0.37	2	B	SD, C	
1187	Sc	11.03	1391	−20.22	0.33	4	B	G, C, R	Grp
1300	Sbc	10.60	1578	−20.97	0.15	7	B	G, C, R	
1365	Sb	9.83	1638	−21.75	0.27	8	G	B	VV 825
1385	Sc	11.01	1497	−20.45	0.17	3	B	G	
1512	Sa	10.75	898	−19.20	0.82	8	G		Grp
1566	SABb	9.98	1502	−21.27	0.32	6	G	B	
1667	SABc	12.22	4567	−21.83	0.09	2	SD	B	
1832	Sbc	10.66	1938	−21.41	0.15	2	B	C	
2336	Sbc	10.63	2202	−22.14	0.17	6	B	G	
2442	Sbc	10.27	1458	−20.91	0.32	5	B	C	Grp
2460	Sab	12.14	1442	−19.78	0.46	3	B		
2528	SABb	13.35	3918	−20.50	0.14	3	SD	B	
2532	SABc	12.65	5248	−21.80	0.29	5	SD	B	
2771	Sab	13.70	5097	−20.74	0.79	7	SD	G, B	
2861	SBbc	13.60	5076	−20.74	0.17	4	SD	B, C	
2989	SABb	12.99	4143	−20.86	0.43	7	HST	B	
3261	Sbc	11.35	2564	−21.34	0.35	6	B	C	
3319	SBc	11.15	742	−19.54	0.24	4	SD	B, C	
3359	Sc	10.75	1013	−20.57	0.36	5	B	G, SD	

Table 1. (Contd.)

NGC/IC	Type	B_0	V_0, km s^{-1}	M_B	M_{HI}/L_B	Number of "row"	Main Reference*	Other References*	Inter-action**
(1)	(2)	(3)	(4)	(5)	(6)	(7)	(8)	(9)	(10)
3408	Sc	14.07	9507	−21.70		3	SD	B, C, R	
3507	SBb	11.86	975	−19.09	0.18	5	SD	B, C	
3513	SBc	11.09	1198	−19.94	0.14	6	B	G, C	
3601	SBab	13.69	8119	−21.68	0.17	4	SD		
3686	SBbc	11.69	1157	−19.63	0.11	5	B	SD, G	
3719	Sbc	13.27	5863	−21.40	0.34	8	SD	B	
3726	Sc	10.31	864	−20.72	0.12	5	B	SD, G, C	
3893	SABc	10.26	962	−21.00	0.10	3	B	SD, G, C	M
3978	SABb	13.14	9950	−22.73	0.14	2	SD	B	
3992	Sbc	10.08	1047	−21.31	0.09	2	B	SD	
4029	SABb	14.02	6197	−20.77	0.21	2	B	SD	
4030	Sbc	10.86	1463	−20.84	0.20	5	SD	G, B	
4035	SABb	13.73	1569	−18.03	0.84	4	B		
4079	SABb	13.27	6086	−21.47	0.21	8	SD	B	
4123	Sc	11.60	1327	−19.91	0.38	2	B	SD, C	
4136	Sc	11.92	590	−18.38	0.27	2	B	SD, C	
4141	SBc	14.35	1900	−18.16	0.71	2	SD	B, C, G	
4145	Scd	11.06	1011	−20.19	0.19	2	B	SD, G	
4151	SABa	11.09	988	−20.16	0.15	2	B		
4156	Sb	13.71	6755	−21.32	1.22	4	SD	B	
4210	Sb	13.20	2713	−19.99	0.14	4	SD	B, C	
4254	Sc	10.18	2408	−22.62	0.19	6	B	SD, G, 2M	
4304	Sbc	12.14	2623	−20.66	0.45	5	B	C	
4319	SBab	12.21	1443	−19.81		1	B		
4444	SABb	12.51	2915	−20.50	0.48	4	C	B	
4450	Sab	10.48	1955	−21.90	0.01	4	G	SD, B	
4475	SBbc	14.01	7388	−21.20	0.32	7	SD	B	
4487	Sc	11.27	1036	−19.67	0.21	2	C	SD, B	
4499	SBbc	13.24	3353	−20.09		3	B	C	
4536	SABb	10.32	1807	−21.85	0.18	7	G	B	
4579	SABb	10.12	1517	−21.74	0.02	3	B	SD	
4603	SABc	11.46	2590	−21.27	0.25	4	B	C	

Table 1. (Contd.)

NGC/IC	Type	B_0	V_0, km s^{-1}	M_B	M_{HI}/L_B	Number of "row"	Main Reference*	Other References*	Inter-action**
(1)	(2)	(3)	(4)	(5)	(6)	(7)	(8)	(9)	(10)
4622	Sa	13.22	4468	−20.77		6	B	C	
4653	SABc	12.61	2624	−20.33	0.46	5	B	SD, C	
4682	SABc	12.35	2322	−20.27	0.19	5	B	SD, C	
4701	Sc	12.45	723	−17.84	0.67	2	SD	B, C	
4734	Sc	13.90	7525	−21.32	0.32	2	SD	B, C	
4736	Sab	8.54	314	−20.98	0.01	6	G	SD	
4897	Sbc	12.87	2558	−19.97	0.87	5	B	G, C	
4902	Sb	11.51	2631	−21.40	0.21	7	B	G, C	
4947	Sb	11.97	2405	−20.65	0.18	6	B	C	
4965	SABc	12.23	2264	−20.27	0.30	8	B	C	
4981	Sbc	11.65	1678	−20.31	0.27	4	B	G	
5020	SABb	12.94	3362	−20.57	0.68	5	SD	G, B	
5033	Sc	10.08	876	−20.95	0.19	4	B	SD, G, C	
5101	S0-a	11.22	1858	−20.84	0.12	4	B		
5112	SBc	12.21	972	−19.04	0.39	2	SD	G, B, C	
5156	SBb	11.74	2986	−21.33	0.22	6	B	2M	
5213	Sb	14.48	6884	−20.55	0.41	2	SD	B, C, R	VV 018, M
5227	Sb	13.60	5235	−20.84	0.41	5	SD	B, C	
5327	Sb	13.15	4354	−20.89	0.33	4	SD	B	
5334	Sc	12.52	1380	−19.12	0.46	3	B	SD, G, C	
5345	Sa	13.34	7255	−21.79	0.10	3	SD	B	
5351	SBb	12.57	3613	−21.16	0.38	6	B	SD, C, 2M	asym
5395	SABb	11.72	3468	−21.92	0.28	5	B	SD, G	VV 048, ARP 084, M
5494	Sc	12.91	2619	−19.93	0.61	6	B	G,	
5584	SABc	12.33	1648	−19.69	0.43	3	B	SD	
5618	SBc	13.40	7140	−21.71	0.34	3	SD	B, C	
5643	Sc	9.95	1190	−21.00	0.10	5	B	C	
5653	Sb	12.69	3564	−20.99	0.12	6	HST	SD, 2M	
5655		16.71				4	B	SD	
5669	SABc	12.41	1373	−19.28	0.57	3	SD	B, C	
5674	SABc	13.06	7473	−22.16	0.15	3	B	SD, C	
5754	SBb	13.74	4404	−20.41	0.32	11	SD	B	ARP 297, M

Table 1. (Contd.)

NGC/IC	Type	B_0	V_0, km s^{-1}	M_B	M_{HI}/L_B	Number of "row"	Main Reference*	Other References*	Inter-action**
(1)	(2)	(3)	(4)	(5)	(6)	(7)	(8)	(9)	(10)
5774	SABc	12.54	1566	−19.37	0.61	1	SD	B, G	M
5786	Sbc		2981			3	B	C	
5850	Sb	11.40	2547	−21.50	0.07	8	G	SD, B	
5861	SABc	11.19	1859	−21.02	0.18	8	B	C	
5905	Sb	12.98	3391	−20.66	1.07	6	SD	G, B, C, R	
5968	SABb	12.50	5460	−21.97	0.21	10	B	C, 2M	
6001	Sc	14.07	9974	−21.79	0.44	5	SD	B, C	
6008	Sb	13.72	4861	−20.60	0.45	4	SD	B, C	
6035	Sc	13.73	4756	−20.55	0.24	4	SD	B, C, 2M	
6217	Sbc	11.46	1368	−20.45	0.27	5	SD	G, B, C	ARP 185
6221	Sc	9.69	1485	−21.70	0.21	4	B	C	
6267	Sc	13.29	2980	−20.04	0.23	3	B	B, C	
6384	SABb	10.55	1664	−21.51	0.19	4	B	SD, C	
6484	Sb	12.73	3114	−20.68	0.66	3	B	SD, C	
6691	Sbc	13.27	5883	−21.50	0.20	2	B	C, 2M	
6699	SABb	12.39	3391	−20.94	0.07	7	B	C	
6744	Sbc	8.61	851	−21.33	1.09	8	G	B, C	Grp, UNGC
6753	Sb	11.51	3176	−21.68	0.17	4	B	G, C	
6769	SABb	12.10	3813	−21.49		6	B	C	VV 304, M
6770	Sb	12.24	3842	−21.37	0.33	3	B	G, C	VV 304, M
6780	SABc	12.90	3493	−20.51	0.25	2	B	C	
6782	Sa	12.18	3923	−21.48	0.11	6	G	B	
6845	SBbc	13.19	6679	−21.69		3	B		
6878	SABb	13.20	5853	−21.40		6	B	C	
6919	SABc	13.26	6727	−21.65		2	C	B, C	
6923	SBb	11.89	2831	−21.11	0.46	4	B	C	
6935	SABa	12.56	4589	−21.48		4	G	C	
6941	Sb	13.48	6219	−21.32	0.43	2	C	SD, B	
6943	Sc	11.45	3116	−21.65	0.43	6	C	G, B	
6949	Sc	12.76	2763	−20.48	0.33	5	C	B	
6951	SABb	10.05	1425	−21.92	0.04	4	C	B	
6955	SABb	14.35	8168	−21.05		5	SD	B, C	

Table 1. (Contd.)

NGC/IC	Type	B_0	V_0, km s^{-1}	M_B	M_{HI}/L_B	Number of "row"	Main Reference*	Other References*	Inter-action**
(1)	(2)	(3)	(4)	(5)	(6)	(7)	(8)	(9)	(10)
6962	SABa	12.37	4202	−21.58	0.33	5	G	SD, B, R	M
6976	SABb	14.35	5998	−20.36		6	SD	B	
6984	Sc	12.66	4663	−21.42	0.40	6	C	B	
7038	SABc	11.94	4932	−22.25	0.34	8	B	C	
7059	SABc	11.56	1734	−20.19	0.70	2	C	B	
7065A	SABc	14.46	7404	−20.70		3	SD	B	
7070	Sc	12.54	2397	−20.00	0.82	4	B	C	
7083	SBbc	11.30	3106	−21.80	0.36	7	B	C	
7102	Sb	13.47	4846	−20.79	0.41	4	B	C	
7125	SABc	12.31	3078	−20.79	1.68	10	B	C	
7171	SBb	12.43	2717	−20.55	0.41	3	B	C	
7221	Sbc	12.41	4356	−21.54	0.30	3	C	B, G	
7252	S0	12.59	4724	−21.54	0.04	5	HST		ARP 226, M
7257	SABb	12.95	4902	−21.31	0.20	4	SD	B, C	
7309	SABc	12.70	4006	−21.10	0.19	5	B	C	
7323	Sb	13.62	5601	−20.98	0.35	2	SD		M
7329	SBbc	12.04	3251	−21.15	0.46	6	C	B, G	
7412	SBb	11.51	1710	−20.25	0.25	4	C	B, G	
7418	Sc	11.42	1447	−19.97	0.27	5	B	C, B	
7421	Sbc	12.41	1801	−19.51	0.15	5	B	C, G	
7424	Sc	10.52	937	−19.78	0.85	5	B	C, G	
7535	Scd	13.95	4604	−20.20	0.65	2	SD	B, C	
7678	Sc	12.04	3488	−21.55	0.16	6	B	C, G, SD, 2M	VV 359, ARP 028
7691	Sbc	13.58	4038	−20.31	0.36	4	SD		
7713A	Sc	12.88	3008	−20.19	0.27	5	C	B	
7714	Sb	12.53	2797	−20.51	0.42	2	SD	B, C	VV 051, ARP 284, M
IC									
0004	Sc	13.69	5011	−20.65	0.17	2	SD	B	
0167	Sc	12.92	2934	−19.39	0.35	4	G	SD	ARP 031
0173	SBbc	14.57	13965	−21.99	0.24	6	SD	B	
0209	SBbc	13.35	3964	−20.41	0.17	2	SD		
0221	Sc	13.13	5088	−21.25	0.46	4	C	B	

Table 1. (Contd.)

NGC/IC	Type	B_0	V_0, km s^{-1}	M_B	M_{HI}/L_B	Number of "row"	Main Reference*	Other References*	Inter-action**
(1)	(2)	(3)	(4)	(5)	(6)	(7)	(8)	(9)	(10)
0342	SABc	6.14	25	−21.54	0.47	7	B	C, R	
0370	Sc	14.39	9727	−21.34	0.52	4	B	C	
0382	SABc	12.74	4998	−21.5	0.53	4	B	C, G	
0438	SABc	12.43	3123	−20.56	0.58	4	C	B, G	
0492	SBbc	13.9	5148	−20.51	0.35	5	SD		
0498	Sb	14.27	10139	−21.59	0.38	2	SD		VV 526
0503	Sa	14	4125	−19.87	1.39	3	SD		
0509	SABc	13.56	5490	−20.98	0.45	5	B	SD	
0512	SABc	12.7	1614	−19.5	0.40	6	G	B	
0527	SBc	14.43	6868	−20.61	0.86	7	SD	B	
0539	Sc	13.97	7043	−21.07	0.29	5	SD	B	
0577	Sc	14.65	9014	−20.95	0.33	6	SD	B	
0616	Sc	14.27	5776	−20.38	0.42	5	SD	B	
0651	SBd	12.9	4491	−21.17	0.28	3	SD		
0900	SABc	13.3	7066	−21.8	0.35	4	SD	C, B	
0983	SBbc	12.49	5442	−22.06	0.67	5	SD	C, B	ARP 117
0992	SABb	14.46	7782	−20.84	0.64	2	SD	B	
1093	SABb	14.5	13370	−21.99	0.47	4	SD	B, G	
1132	Sc	14.07	4524	−20.1	0.65	5	SD	C, B	
1142	SBc	14.51	13973	−22.09	0.70	4	SD	C, B, 2M	M
1149	Sbc	13.76	4681	−20.47	0.41	4	SD	C, B	M
1236	Sc	13.79	6026	−20.99	0.29	3	SD	C, B	VV 442, M
1269	Sbc	12.7	6115	−22.11	0.26	6	B	C	
1301	Sc	14.1	3990	−19.86	1.36	3	C	B	
1377	SBab	14.22	9039	−21.4		5	SD		
1516	Sbc	13.83	7278	−21.29	1.08	7	SD	B	
1525	Sb	12.52	5010	−21.89	0.31	5	B	C	
1543	Sbc	13.94	5595	−20.65	0.36	2	SD	B	
1562	SBc	13.46	3728	−20.12	0.65	4	C	B	
1607	Sc	14.14	5438	−20.34	0.66	3	SD		
1666	Sc	14.1	4881	−20.2	0.38	2	B	SD	
1734	Sc	13.29	4924	−20.9	0.34	3	B		

Table 1. (Contd.)

NGC/IC	Type	B_0	V_0, km s^{-1}	M_B	M_{HI}/L_B	Number of "row"	Main Reference*	Other References*	Inter-action**
(1)	(2)	(3)	(4)	(5)	(6)	(7)	(8)	(9)	(10)
1764	Sb	13.81	5066	−20.56	0.45	5	B	C	
1852	Sc	14	8428	−21.45		4	B		
1953	Sc	11.76	1864	−20.21	0.15	2	B		
2226	SABa	13.88	10876	−22.14	0.13	5	SD	B	
2473	Sbc	14.32	8070	−21.07	0.31	3	G		
2490	SABb	14.3	7333	−20.88	0.97	4	SD		
2522	Sc	12.44	3017	−20.32	0.61	2	B	G, C	
2537	Sc	12.11	2788	−20.65	0.34	4	B	G	
2548	SBbc	13.18	4409	−20.77	0.39	6	B	C	
2556	Scd	13.37	2505	−19.46	0.47	2	B	C	
2580	Sc	12.93	3140	−20.26	0.51	6	B	C, R	
2582	Sbc	13.32	4161	−20.5	0.21	7	B	C, R	
2604	SBm	14.5	1628	−17.57	1.75	1	SD	B, C, R	VV 538, M
2627	SABc	11.89	2088	−20.41	0.28	5	B	G, C, 2M	
2947	SBm	14.3	12705	−22.08	0.45	3	SD	B	asym
2956	Sbc	14.62	9056	−21.02	0.47	5	B	SD	
3062	Sc	14.32	7860	−21	0.31	5	SD	B	
3109	Sbc	14.46	12853	−21.93	0.37	4	SD	B	
3115	Sc	13.3	734	−18.64	0.37	6	B	G	VV 431, Grp
3156	SBcd	14.33	5874	−20.37	0.30	2	B	SD	
3253	Sc	11.62	2706	−20.65	0.24	3	B	C	
3267	Sc	13.99	1236	−18.87	0.20	5	SD	B	
3271	SABc	14.42	7211	−20.71	0.52	3	SD	B, C	M
3376	SBa	14.07	7130	−21.06	0.65	2	SD	B	
3407	SBb	14.14	7004	−20.95	0.31	3	B	SD	
3709	Sbc	14.68	14311	−21.95	0.61	4	SD	B	
3827	Sc	13.58	4303	−20.39	0.29	4	B		
3829	SABa	13.26	3564	−20.25	0.74	4	B	C	
3896A	Scd	11.88	2142	−20.42	0.13	1	B	C	
4219	SBb	13.18	3654	−20.38	0.14	2	B	2M	
4229	Sb	14.16	6953	−20.89	0.46	2	SD	B, C	M
4237	SBb	12.48	2658	−19.87	0.24	4	B	C	

Table 1. (Contd.)

NGC/IC	Type	B_0	V_0, km s^{-1}	M_B	M_{HI}/L_B	Number of "row"	Main Reference*	Other References*	Inter-action**
(1)	(2)	(3)	(4)	(5)	(6)	(7)	(8)	(9)	(10)
4248	Sc	13.51	4105	−20.31	0.74	4	B		
4270	Sbc	14.16	7964	−21.13	0.70	5	B	C	
4341	Sc	14.64	2344	−18.24	1.96	4	B	SD	
4359	Sc	13.16	4130	−20.64	0.54	3	B	C, 2M	
4366	Sc	12.75	4615	−21.32	0.31	5	B	C	
4367	SABc	12.54	4054	−21.24	0.23	6	B	C	
4388	Sbc	13.79	4010	−19.99	0.59	3	B		
4397	Sbc	13.7	4381	−20.41	0.52	5	SD	B	
4441	Sc	13.65	4452	−20.34	0.45	2	B	C	Grp
4444	SABb	11.2	1958	−20.91	0.13	5	B	2M	
4479	Sc	14.67	13593	−21.86	0.64	3	SD	B, C	
4538	SABc	12.13	2862	−20.94	0.12	5	B	C	
4567	Sc	13.24	5728	−21.31	0.21	4	SD	2M	M
4585	SBb	12.05	3645	−21.46		6	B	C	
4633	Sc	12.14	2942	−20.44	0.56	6	B	C	
4641	Sc	13.7	5333	−20.64	0.16	7	B	C	
4646	Sc	11.83	3172	−21.36	0.53	6	B	C, 2M	
4661	Sc	12.95	4828	−21.16	0.61	5	B	C	
4682	SBbc	12.38	3570	−21.05	0.47	4	B	C	
4688	Sc	13.71	6026	−21.05	0.21	3	B	SD	
4722	Sc	12.83	4817	−21.3		6	B		
4729	Sc	12.44	4434	−21.49	0.29	8	B	C	
4769	SBbc	13.26	4535	−20.73	0.60	5	B	C	
4836	SBc	12.82	4604	−21.21	1.07	5	B	G, 2M	
4839	Sbc	12.77	2717	−20.07	0.50	6	B	M	
4852	SBc	12.84	4425	−21.09	0.36	5	B	C	
4857	Sc	12.94	4674	−21.13	0.38	3	B	C	
4876	SABc	13.7	5577	−20.78	0.63	5	B	C	
4901	SABc	11.44	2139	−20.11	0.37	9	B	C	
4933	SBbc	12.4	4910	−21.79	0.37	4	B	G	
4998	SBc	13.42	6662	−21.48		4	B	C	
5005	SBc	13.06	3094	−20.16	0.71	6	C	B	

Table 1. (Contd.)

NGC/IC	Type	B_0	V_0, km s^{-1}	M_B	M_{HI}/L_B	Number of "row"	Main Reference*	Other References*	Inter-action**
(1)	(2)	(3)	(4)	(5)	(6)	(7)	(8)	(9)	(10)
5092	SBc	12.74	3246	−20.48	0.42	9	B		
5116	SBbc	13.6	3791	−19.97	0.47	3	B	C	
5141	Sbc	13.09	4477	−20.86	0.64	4	B	C	
5188	SABc	13.47	4614	−20.55	0.47	5	B	C	M, Grp
5261	SBc	13.56	3238	−19.74	0.46	4	B	C	
5325	Sbc	11.71	1507	−19.75	0.12	8	C	G, 2M	

* Abbreviations: C — DSS colored; 2M — 2MASS;
B — DSS2 Blue (XJ+S); G — GALEX;
R — DSS2 Red (F+R); SD — SDSS DR9 color;
HST — Hubble Space Telescope (optical).

** Remarks: VV — the number of the object in the Vorontsov-Velyaminov catalog;
ARP — the number of the object in the catalog of peculiar galaxies;
M — the object belongs to a pair or a group of galaxies according to HyperLeda data;
Grp — the object is included in the catalog of Makarov and Karachentsev [8];
UNGC — the object is included into the catalog of Karachentsev et al. [9] and has large tidal index ($\Theta \geqslant 2.0$);
asym — the object is asymmetric with pronounced signs of interaction.

2.2. Statistical Properties

To analyze the possibility of merging our sample with that of catalog [3], we identified "rows" in six randomly selected objects from [3] using the corresponding SDSS/DSS images instead of the Palomar Atlas images and found our results to differ appreciably from those of Chernin et al. in terms of the number of "rows" (Table 2) for all objects except for NGC 1637. The discrepancy is most significant in the case of NGC 5921, and this can be explained by the fact that modern images of the central region of the galaxy have higher resolution unattainable with Palomar Atlas images. In view of this result, which is due to the large difference between the quality of initial observational data, we consider it unfeasible to merge the samples in order to analyze the distributions of the number of "rows", their linear and angular sizes.

At the same time, the distributions of other properties of galaxies with polygonal structures from [3] agree well with the corresponding distributions reported in this paper, and we show them both separately (for the sample from [3] with the updated parameter values from HyperLeda database, and for our sample) and for the combined sample.

Let us now compare the statistical properties of our sample with the results of Chernin et al. [3]. Figure 2 shows the distributions of morphological types. This distribution for our galaxy is slightly shifted toward earlier-type galaxies compared to the corresponding distribution in [3]. Figs. 3a and 3b show the distributions of absolute magnitudes of galaxies for the two catalogs. The absolute magnitudes of objects of our sample lie in the interval from $-17^{\rm m}$ to $-22\overset{\rm m}{.}5$ with a mean of $M_B = 20\overset{\rm m}{.}5$ both for the entire sample and for barred galaxies, which is consistent with the results of [3].

According HyperLeda data, 77% of the galaxies of our sample are barred. The fraction of barred galaxies in catalog [3] is equal to 70%, resulting in a 74% fraction of SB galaxies among the combined sample of all 406 NGC/IC objects with "rows". However, HyperLeda indicates the presence of a bar in 51% of all 7 143 NGC/IC galaxies. The presence of a bar appears to be a favorable factor for the formation of polygonal structures in the spiral density wave due to more suitable conditions for the development of

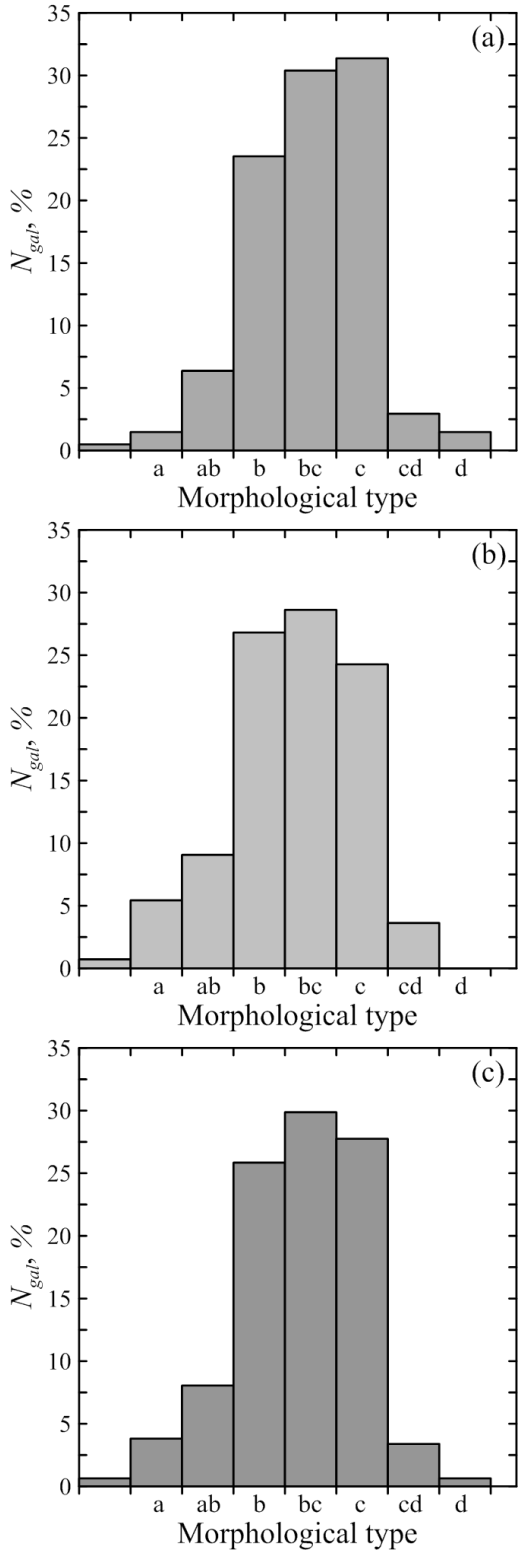

Fig. 2. Distribution of morphological types of galaxies: (a) for the sample of Chernin et al. [3] updated with information from the HyperLeda database; (b) for our sample of galaxies; (c) combined histogram for the merged sample.

Table 2. Number of "rows" in randomly selected galaxies from the catalog of Chernin et al. [3] found by inspecting Palomar Atlas and SDSS/DSS images

Galaxy	Number of "rows" according to [3]	Our estimate of the number "of rows"
NGC 0514	2	4
NGC 1637	3	3
NGC 5597	2	4
NGC 5921	3	8
NGC 7229	2	3
NGC 7755	4	5

strong galactic shocks (GS) in the stronger potential of the stellar density wave.

The number of "rows" N in galaxies of our catalog varies from one to 11 with a mean of $\langle N\rangle = 4$ (Fig. 4). In the case of catalog [3] the average number of "rows" for the entire sample is close to three with two or three "rows" found in most of the galaxies. The distribution of the number of "rows" in our sample is rather broad with a less pronounced maximum (see Fig. 4b). Like in the catalog of Chernin et al. [3], we found no correlation between the number of "rows" and absolute magnitude M_B.

Linear sizes of "rows", L, vary over a wide range, exceeding 22 kpc in several galaxies, e.g., NGC 0010, NGC 1365, NGC 1512, NGC 3976, NGC 5850, and NGC 6935, and reaching 30 kpc in IC 4479 (Fig. 5). The average length of a "row" is $\langle L\rangle = 6.6$ kpc, and the median length is 5.6 kpc. These results are almost twice the values for catalog [3]. This discrepancy is due to (1) higher fraction of long "rows" because our analysis reveals more extended spiral structure and (2) because of the increase of L with galactocentric distance r combined with high quality of SDSS images of peripheral parts of galaxies and the fact GALEX images allow tracing spiral structure far beyond the optical radius.

Like in the case of catalog [3], we find the length of the "row" to correlate with galactocentric distance d of the end of the "row": the farther from the center, the longer the "rows" (Fig. 6). The length of the "row" and galactocentric distance d are normalized to the optical radius of the galaxy, $D_{25}/2$. The solid line in Fig. 6 shows the dependence $d = L$, and the dashed line, the linear approximation of this dependence, $d = 0.87L + 0.1$.

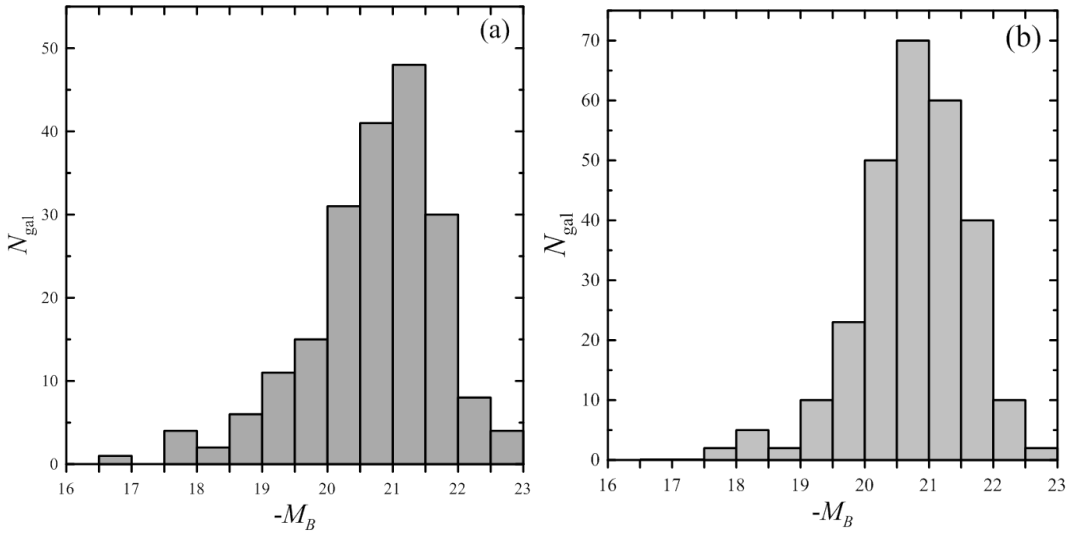

Fig. 3. Distribution of absolute magnitudes of galaxies: (a) for all galaxies of the sample of Chernin et al. [3]; (b) for our sample of galaxies.

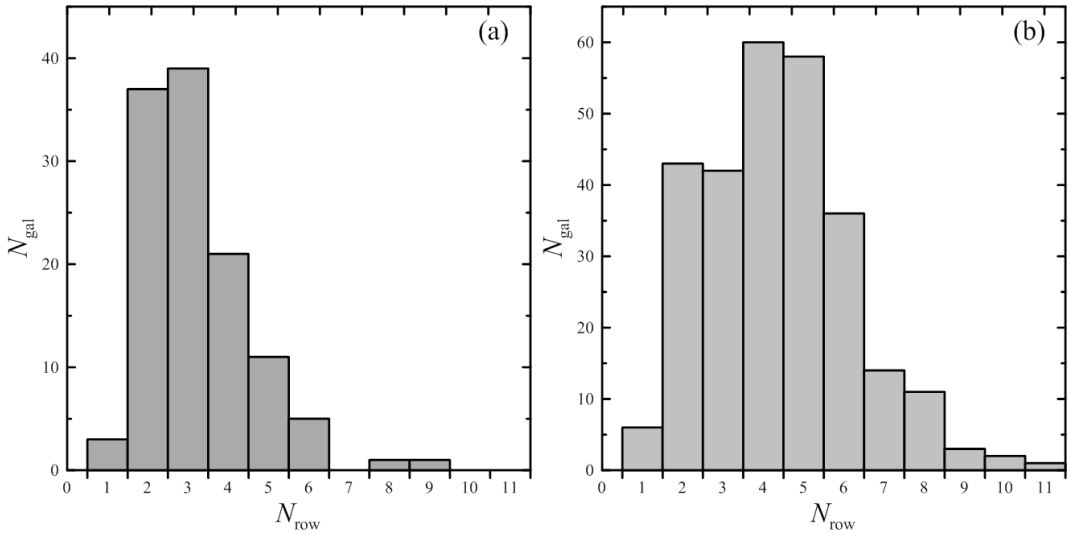

Fig. 4. Same as Fig. 3, but for the number of "rows".

Figure 7 shows the distributions of inclination i for galaxies with "rows" (7a) and for all S-type NGC and IC galaxies according to HyperLeda data. The entire sample of NGC/IC galaxies contains a large fraction of objects with inclinations $i \simeq 90°$, which is due to the effect of higher surface brightness of edge-on galaxies resulting from geometric factor. There is also an extra contribution due to $i = 90°$ being assigned to some non-disk galaxies in the HyperLeda database. The fraction of polygonal galaxies with inclinations $i > 70°$ is small because of the problems with the determination of the properties of the spiral pattern, and we exclude these objects from consideration.

Figure 7 demonstrates the qualitative similarity of galaxies with "rows" and all S-type NGC and IC galaxies as far as the distribution of inclinations i is concerned. In both cases we have a bell-shaped distribution with a maximum near 40° for galaxies with "rows" and 50° for all S-type galaxies. The non-uniformity of the distribution is due to observational selection and the method used to determine inclination based on the photometric axis ratio b:a. Because of the presence of the bar, bulge, and various shape distortions in interacting galaxies and objects of late morphological types such axial-ratio based estimates should evidently result in systematic deviations from uniform distributions both for galaxies with small (face-on) and large (edge-on) inclinations i [10].

Straight-line segments are difficult to identify in galaxies with large inclination and that us why, given

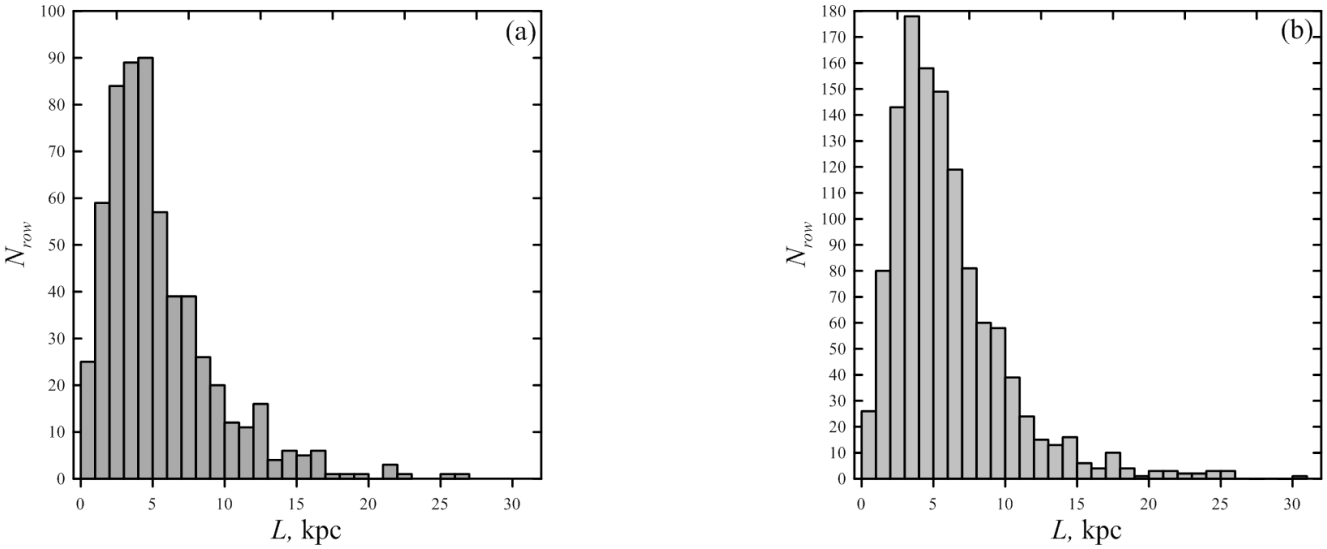

Fig. 5. Distribution of linear sizes of "rows": (a) for all galaxies from the sample of Chernin et al. [3]; (b) for our sample of galaxies.

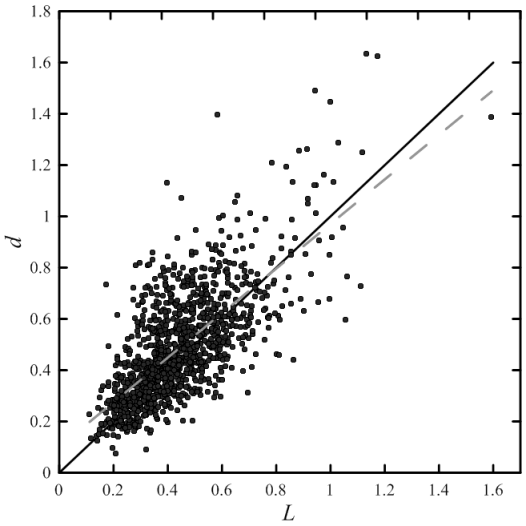

Fig. 6. The "row length L — galactocentric distance d" diagram (both quantities are normalized to the optical radius of the galaxy, $D_{25}/2$). The dashed and solid lines show the regression relation and the identity relation $d = L$, respectively.

the incompleteness of our sample, hereafter for inclinations $i \geqslant 55°$ (see Fig. 7) we show the distributions for both the combined sample of galaxies with "rows", and separately for galaxies with $i < 55°$.

The angle between the adjacent "rows" is usually close to $\alpha = 120°$ (Fig. 8). The average angle is equal to 126° both for our entire sample and for barred galaxies, in agreement with the result of Chernin et al. [3].

Figure 9 shows the estimates of gas content in galaxies with "rows": the distributions of the $M_{\rm HI}/L_B$ ratio (in solar units). The maximum is at 0.3 and the mean ratio for the entire sample is $\langle M_{\rm HI}/L_B \rangle = 0.39$, which is consistent with the results of [3].

According to HyperLeda, UBV photometry with color indices corrected for selective Galactic extinction and galaxy disk inclination is available for 34% of the galaxies with "rows" from our catalog. Figure 10 shows the $(U-B)_0$–$(B-V)_0$ color-color diagram, where diamond symbols indicate updated data or the sample of Chernin et al. [3], and the crosses and circles show the positions of objects of our sample. The data points for all galaxies with "rows" agree well with the intrinsic color relation, which is shown by the solid line.

3. FORMATION MECHANISMS OF POLYGONAL STRUCTURES

Two possible formation mechanisms for polygonal structures have been discussed in the literature. Chernin [11, 12] proposed hydrodynamical mechanism based on particularities of the dynamics of the global galactic shock. Because of the instability of the shock front it tends to become locally flat and polygonal structure forms. This mechanism is bona fide reproduced in numerical simulations of various authors [13–17].

Another mechanism is also possible where individual straight-line arm segments can be recognized in numerical N-body models at the stage of the formation of the transient bar [5]. Models based on the 4/1 resonance can also describe the observed features of the spiral structure [18, 19]. The mechanism of the formation of "rows" based on the gravitational instability of the collisionless stellar disk

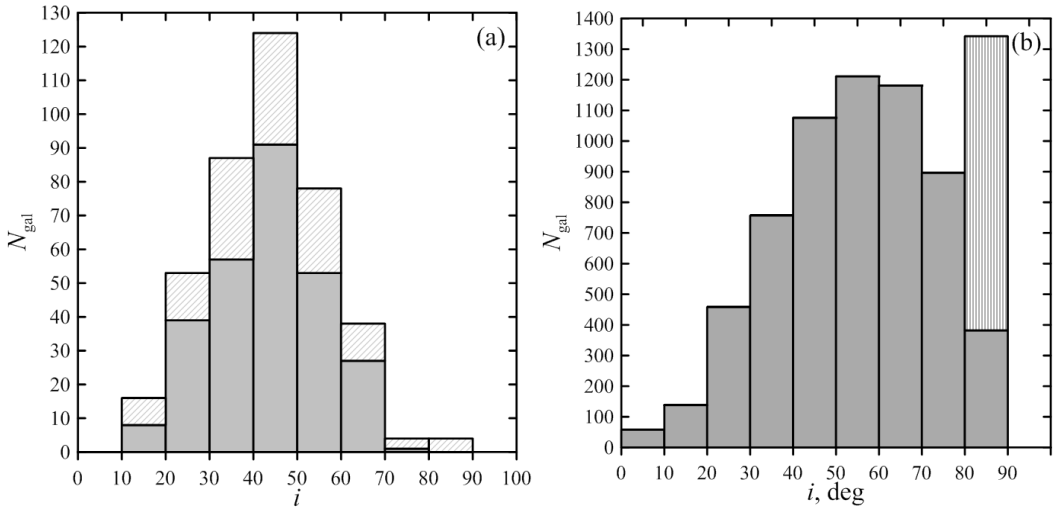

Fig. 7. Distribution of inclinations i of spiral galaxies: (a) for NGC and IC galaxies with "rows" (276 objects of our catalog—the shaded bars, 406 objects including NGC objects from the catalog of Chernin et al. [3]—the dashed bars); (b) for all spiral galaxies of the NGC/IC catalogs (according to HyperLeda data); the stripped bar—fir those with $i \geq 90°$.

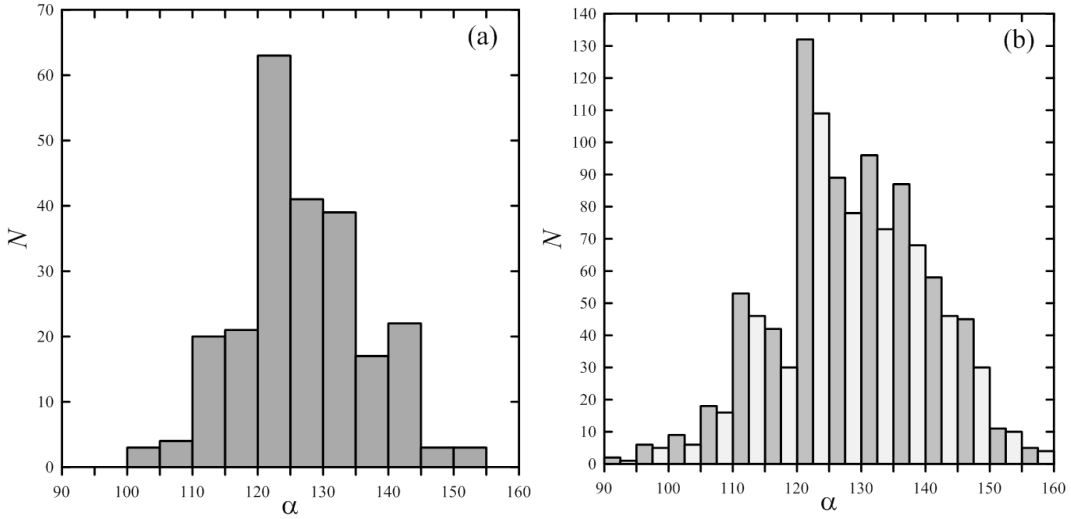

Fig. 8. Histogram of the distribution of angles α between the adjacent "rows": (a) for all galaxies of sample [3]; (b) for our sample of galaxies. The light-shaded bars show the distribution for galaxies with $i < 55°$.

and/or on resonance phenomena was analyzed by Rautiainen et al. [20], Rautiainen and Melnik [21], and Melnik and Rautiainen [22]. When constructing their numerical models of stellar disks the above authors used gravitational potentials constructed from H-band photometry of the OSUBSGS (Ohio State University Bright Spiral Galaxy Survey) survey. They could reproduce straight-line segments in terms of a collisionless N-body model, in particular, for the NGC 4303 galaxy.

Let us now point out some distinctive features in stellar disks according to the results of our dynamic N-body simulations without going into details of particular physical mechanisms of the formation of "rows" [21, 22]. A detailed description of the numerical model employed can be found in [23, 24]. Straight-line segments appear in models with sufficiently massive halos with $\mu = M_h/M_d \gtrsim 3$ within the optical radius. Only in such models multi-armed and sufficiently narrow spirals with recognizable transient straight-line segments ("rows") can form at various values of the Toomre parameter $Q_T \lesssim 1$. Figure 11 shows the results of our numerical N-body models where straight-line arm segments and even almost kink points can be seen. Let us point out some of the features of models of stellar disks with "rows":

• Straight-line spiral segments are non-stationary, like in the case of "rows" in a gaseous disk.

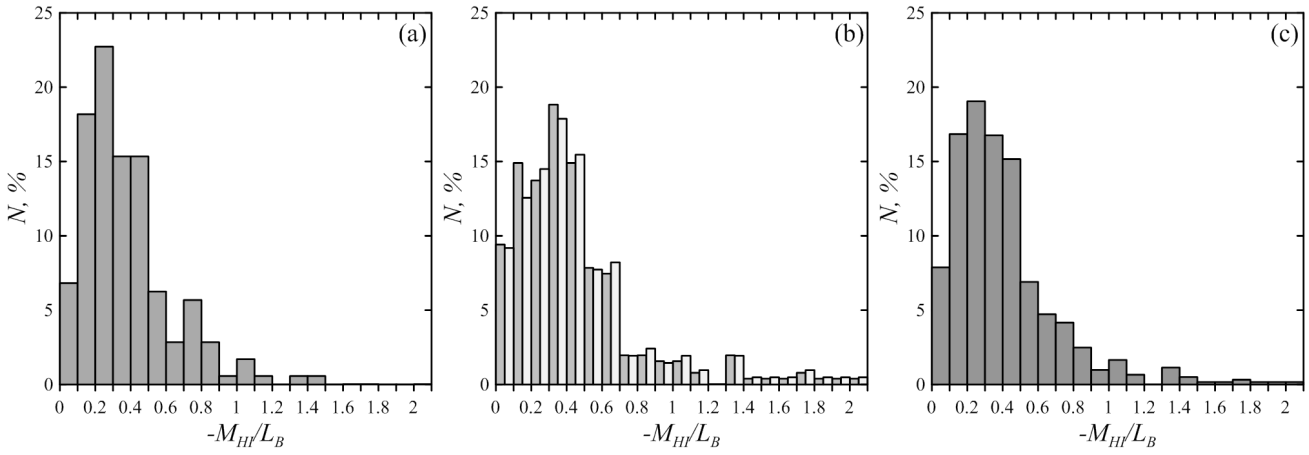

Fig. 9. Distribution of the $-M_{HI}/L_B$ ratio (in solar units) for galaxies with "rows": (a) for the full sample of Chernin et al. [3] updated with data from HyperLeda; (b) for our sample (the light-shaded bars show the distribution for galaxies with inclinations $i < 55^\circ$); (c) the combined histogram for all objects with polygonal structures.

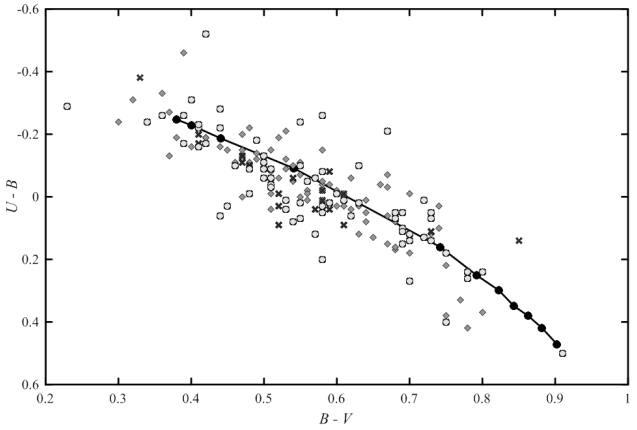

Fig. 10. Color-color diagram for galaxies with "rows": the diamond symbols show the data for the full sample of Chernin et al. [3]; the circles and crosses show the objects of our sample with $i < 55^\circ$ and $i \geqslant 55^\circ$, respectively. The color indices are corrected for selective Galactic extinction and galaxy disk inclination. Actual data from HyperLeda are used.

However, their lifetime scales in hot collisionless medium are appreciably shorter than in gas;

- These structures arise rather seldom and for a short time, usually during the initial stages of the development of gravitational instability;
- Polygonal structure consists of one to three "rows", unlike what we have in gas-dynamic models, where a global system of "rows" forms.

We already pointed out that according to 2MASS data, "rows" occur rather rarely in old stellar disks (see Subsection 2.1). Straight-line segments can be recognized in 2MASS images of 18 objects of our sample, and this fact is indicative of the large amplitude of the spiral wave in the massive stellar disk. One would hardly expect perturbation in gas (whose mass is, on the average, small compared to the mass of stars) to be able to build up a "row" in the old stellar component. The problem is further complicated by the non-stationary (transient) nature of the polygonal structure: under these conditions the time scale of the gravitational influence of the gaseous structure on the stellar component may be insufficient. In the case of the 13 galaxies mentioned above the primary formation mechanism of "rows" in the stellar component must be the stellar disk itself, although this hypothesis does not rule out subsequent parallel operation of the hydrodynamical mechanism.

In many cases "rows" can be identified with the locations of giant molecular clouds and stellar complexes whose formation is associated with the stellar density wave and Galactic shocks [25–28]. Chernin [11, 12] analyzed the gas-dynamic mechanism of the formation of the polygonal structure based on properties 1 and 2 of the Section 1. A number of studies [13–17] used numerical simulations to tackle the problem of the formation of straight-line segments in the gaseous disk of the galaxy in the gravitational potential of a smooth spiral wave, and the results of these studies agree practically with all the observed properties of galaxies with "rows".

After the development of the global shock in numerical models its front becomes unstable, the shock moves out of the spiral gravitational wave and the front becomes flat. As a result, the straight segments of the shock form a polygonal structure with the properties similar to those observed in real galaxies [13]. Our analysis makes it possible to identify objects where apparently only the gas-dynamic mechanism is operating. This is primarily true for objects where the spiral arms and "rows" in GALEX images extend beyond the stellar disk. Furthermore, one to two "rows"

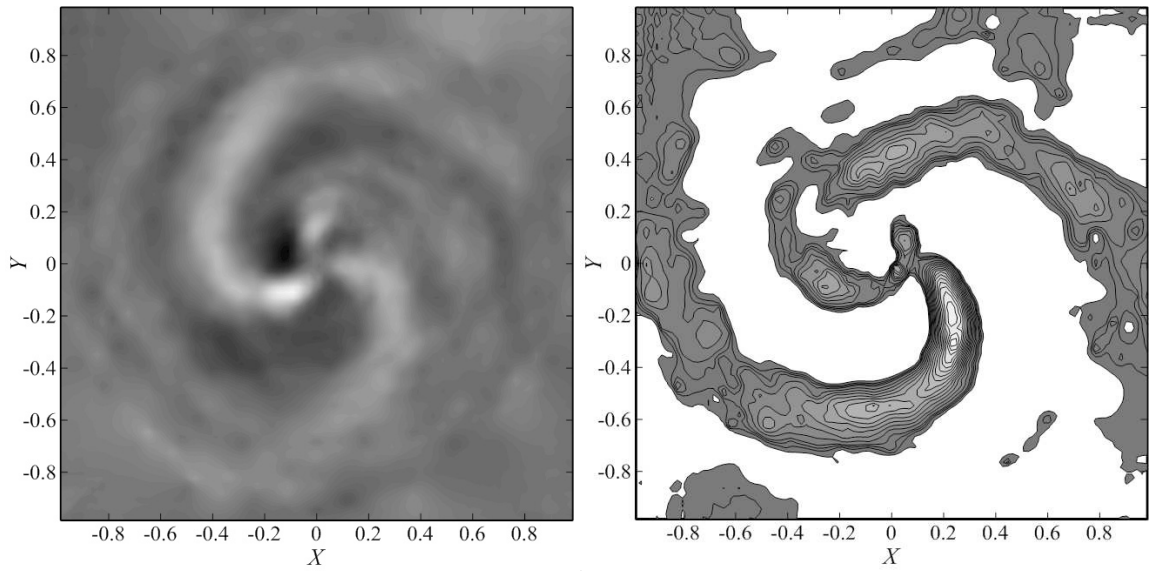

Fig. 11. Distribution of the perturbation of surface density logarithm in the model stellar disk at different time instants (the left-hand panel shows only the positive part of the perturbation). At the initial time instant the Toomre parameter in the region $1/2 \lesssim r/r_d \lesssim 2$ is $Q_T = 0.8$, where r_d is the exponential disk scale.

can usually be found in a single arm in 2MASS images of the old stellar disk (only in NGC 4303 a kink can be seen in each of the three arms, whereas three or more segments in a single arm can be recognized only in the NGC 5156 and IC 5325 galaxies). The gasdynamic mechanism appears to dominate in galaxies with many "rows".

4. DISCUSSION AND CONCLUSIONS

In this study we found 276 more NGC and IC objects with straight-line segments of spiral arms in addition to those listed in the catalog of galaxies with "rows" compiled by Chernin et al. [3]. Together with the 130 NGC objects from catalog [3] they make up a combined sample of 406 galaxies. Unlike Chernin et al. [3], whose catalog is based on an analysis of Palomar Atlas objects, we analyzed all NGC/IC galaxies thereby ensuring the completeness of our sample subject to additional constraints on the observed properties. An analysis of the images of all 7143 NGC/IC spiral galaxies allowed us to find at least one "row" in the structure of the spiral pattern of 406 objects. Thus the occurrence frequency of galaxies with "rows" among the nearest objects is of about 6%. Of these, 77% have central bars. A substantial fraction (38%) of objects with "rows" have rings. Note that 13 (4%) objects are included into the catalog of early-type galaxies with outer rings [29] (nine of them are included in our sample and four objects are listed in catalog [3]).

Unlike objects of the catalog of Chernin et al. [3], where the fraction of interacting galaxies amounts to 44% (90 objects), our sample contains only about 13.8% (38 objects) interacting or highly asymmetric systems. As a result, the combined sample of all 480 objects with "rows" contains only 128 interacting galaxies (27%). Hence the hypothesis of Chernin et al. [3] that interacting galaxies occur almost twice more often among galaxies with "rows" is not supported by the analysis of the combined sample of 480 objects.

Of the 276 new objects 232 galaxies (84%) have two-armed spiral pattern, 8% have three arms, and about 8% galaxies have more than three arms. Only 12 objects (4.3%) exhibit well-defined flocculent spiral pattern, and the corresponding fraction is also low in sample [3]. "Rows" in all arms were found only in 59% of our polygonal galaxies, 28% galaxies (78 objects) have "rows" only in one arm.

We used optical images to schematically outline the "rows" in spiral arms and perform subsequent measurements of linear and angular sizes in most of the galaxies of our sample (93%). DSS images were the main source for identifying polygonal structures for 164 objects (59%): DSS2 Blue (XJ+S) for 145 objects and DSS colored (composite color DSS image) for 19 objects. SDSS DR9 color images are used to construct images of "rows" for 89 objects (32%) of our sample. In four galaxies the "rows" are best recognized in optical images of the Hubble Space Telescope (HST). Only for 19 galaxies (7%) of our entire sample we used GALEX data as the main images for recognizing polygonal structures, however, "rows" could be recognized in ultraviolet

in 51 (18%) galaxies of our sample. In the infrared (2MASS) straight-line segments of spiral arms can be recognized in 18 (7%) objects, these images usually reveal one to two "rows", whereas more such structures can be seen in optical or ultraviolet images. Note also that red DSS images (DSS2 Red (F+R)) reveal "rows" only for 13 objects of our sample.

Except for our estimate of the fraction of interacting galaxies all other statistical properties of our sample agree well with the results of the analysis of the catalog of Chernin et al. [3]. The hypothesis about high gas content in galaxies with "rows" proposed by Chernin et al. [3] argues for hydrodynamical mechanism of the formation of straight-line segments due to the instability of powerful shocks, which agrees with the results of numerical simulations [13–17]. Numerical models suggest transient nature of the formation of polygonal structures, which arise and disappear during the evolution of the galactic disk. The data for our sample also qualitatively suggest that "rows" are non-stationary, because the spiral pattern in about 40% of the galaxies does not form any regular geometric structure.

Note also that the number of "rows" in galaxies of our sample is, on the average, appreciably greater than in catalog [3]. This, in turn, is due to the use of images from more recent digital surveys taken in various wavelength ranges, unlike the analysis of Chernin et al. [3], which was based on a homogeneous sample of blue images from the Palomar atlas.

ACKNOWLEDGMENTS

This paper uses information contained in HyperLeda astronomical database. We are grateful to the reviewers and D. I. Makarov for valuable and useful discussions. This work was supported by the project within the framework of government contract from by the Ministry of Education and Science of the Russian Federation (project No. 2.852.2017/4.6) and partially supported by the Russian Foundation for Basic Research (grants no.s 15-02-06204, 15-52-12387, and 16-02-00649). M. A. Butenko thanks N. M. Kuz'min for assistance.

REFERENCES

1. B. A. Vorontsov-Velyaminov, Astron. Zh. **41**, 814 (1964).
2. A. D. Chernin, A. V. Zasov, V. P. Arkhipova, and A. S. Kravtsova, Astron. Astroph. Transactions **20**, 139 (2001).
3. A. D. Chernin, A. S. Kravtsova, A. V. Zasov, and V. P. Arkhipova, Astronomy Reports **45**, 841 (2001).
4. A. D. Chernin, A. V. Zasov, V. P. Arkhipova, and A. S. Kravtsova, Astronomy Letters **26**, 285 (2000).
5. R. Buta and F. Combes, Fund. Cosmic. Physics **17**, 95 (1996).
6. M. A. Butenko, Vestnik Volgogr. Gos. Univ. Ser. 1: Matematika. Fizika **1**, 52 (2015).
7. D. Makarov, P. Prugniel, N. Terekhova, et al., Astron. and Astrophys. **570**, A13 (2014).
8. D. Makarov and I. Karachentsev, Monthly Notices Royal Astron. Soc. **412**, 2498 (2011).
9. I. D. Karachentsev, D. I. Makarov, and E. I. Kaisina, Astron. J. **145**, 101 (2013).
10. V. E. Karachentseva, Y. N. Kudrya, I. D. Karachentsev, et al., Astrophysical Bulletin **71**, 1 (2016).
11. A. D. Chernin, Astron. Astroph. Transactions **18**, 393 (1999).
12. A. D. Chernin, Monthly Notices Royal Astron. Soc. **308**, 321 (1999).
13. S. A. Khoperskov, A. V. Khoperskov, M. A. Eremin, and M. A. Butenko, Astronomy Letters **37**, 563 (2011).
14. S. A. Khoperskov, M. A. Eremin, and A. V. Khoperskov, Astron. Astroph. Transactions **27**, 245 (2012).
15. E. A. Filistov, Astronomy Reports **56**, 9 (2012).
16. E. A. Filistov, Astronomy Reports **59**, 118 (2015).
17. M. A. Butenko and S. A. Khoperskov, Vestnik Vogogr. Gos. Univ. Ser. 1: Matematika. Fizika **1 (14)**, 81 (2011).
18. G. Contopoulos and P. Grosbol, Astron. and Astrophys. **155**, 11 (1986).
19. P. A. Patsis, P. Grosbol, and N. Hiotelis, Astron. and Astrophys. **323**, 762 (1997).
20. P. Rautiainen, H. Salo, and E. Laurikainen, Monthly Notices Royal Astron. Soc. **388**, 1803 (2008).
21. P. Rautiainen and A. M. Mel'Nik, Astron. and Astrophys. **519**, A70 (2010).
22. A. M. Melnik and P. Rautiainen, Monthly Notices Royal Astron. Soc. **434**, 1362 (2013).
23. A. Khoperskov, D. Bizyaev, N. Tiurina, and M. Butenko, Astronomische Nachrichten **331**, 731 (2010).
24. S. A. Khoperskov, A. V. Khoperskov, I. S. Khrykin, et al., Monthly Notices Royal Astron. Soc. **427**, 1983 (2012).
25. Y. N. Efremov, Monthly Notices Royal Astron. Soc. **405**, 1531 (2010).
26. A. S. Gusev, F. Sakhibov, and Y. N. Efremov, Astronomische Nachrichten **336**, 401 (2015).
27. Y. N. Efremov, Astron. Astroph. Transactions **29**, 25 (2015).
28. N. Bastian, M. Gieles, Y. N. Efremov, and H. J. G. L. M. Lamers, Astron. and Astrophys. **443**, 79 (2005).
29. I. P. Kostiuk and O. K. Silchenko, Astrophysical Bulletin **70**, 280 (2015).

Translated by A. Dambis